

Umut Topal*

Frequency optimization of laminated composite spherical shells

Abstract: This paper deals with frequency optimization of symmetrically laminated angle-ply spherical shells. The design objective is the maximization of the fundamental frequency, and the design variable is the fiber orientation in the layers. The first-order shear deformation theory and nine-node isoparametric finite element model are used for the finite element solution of the laminates. The modified feasible direction (MFD) method is used for the optimization routine. For this purpose, a program based on FORTRAN is used. Finally, the numerical analysis is carried out to investigate the effects of geometrical parameters and boundary conditions on the optimal designs, and the results are compared.

Keywords: fundamental frequency; laminated spherical shells; modified feasible direction method; optimization.

*Corresponding author: Umut Topal, Faculty of Technology, Department of Civil Engineering, Karadeniz Technical University, Trabzon, Turkey, e-mail: umut@ktu.edu.tr

1 Introduction

Laminated composite plates and shells are extensively used in the constructions of aerospace, civil, marine, automotive, and other high-performance structures due to their excellent mechanical properties, such as high stiffness-to-weight ratio, high strength-to-weight ratio, excellent fatigue resistance, improved thermal characteristics, and long-term durability. The increasing application of the fiber-reinforced composite materials has resulted in a renewed interest in the vibration of composite plates and shells at large amplitude. These structures invariably experience severe dynamic environments during service and undergo flexural oscillations with amplitudes comparable to or larger than the thickness of the plate/shell inducing significant geometric non-linearity.

A considerable amount of literature exists on the vibration of laminated spherical shells. For example, Narasimhan and Alwar [1] presented analytical solutions for the free vibration of laminated orthotropic spherical shells. The analysis was based on the application of the

Chebyshev-Galerkin spectral method for the evaluation of free vibration frequencies and mode shapes. Xu and Chia [2] investigated the dynamic non-linear axisymmetric response of a shallow spherical shell with a circular opening at the apex. Xu and Chia [3] studied the non-linear vibration of symmetrically laminated thin spherical caps with flexible supports based on a non-linear theory. Hashemi et al. [4] investigated closed-form solutions for in-plane and out-of-plane free vibration of moderately thick laminated transversely isotropic spherical shell panels on the basis of Sanders theory without any usage of approximate methods. Lee and Chung [5] developed a finite element model of vibrating laminated spherical shell panels with delamination around a central cutout based on the third-order shear deformation theory of Sanders. Nanda and Bandyopadhyay [6] investigated the large-amplitude free flexural vibration of doubly curved shallow shells in the presence of cutouts. Stavsky and Greenberg [7] studied the three-dimensional elasticity problem of the radial vibrations of a composite hollow spherical shell laminated with spherically orthotropic layers. Panda and Singh [8] analyzed the nonlinear free vibration behavior of a thermally postbuckled laminated composite spherical shallow shell panel. Hashemi and Fadaee [9] presented a new exact closed-form procedure for the free vibration analysis of a moderately thick spherical shell panel based on the first-order shear deformation theory. Topal [10] studied mode-frequency analysis of a simply supported equal-sided sector of a laminated spherical shell.

To the best of the author's knowledge, frequency optimization of laminated composite spherical shells has not been investigated yet. Therefore, in this study, frequency optimization of symmetrically laminated spherical shells is investigated to fill this gap. The design objective is the maximization of the fundamental frequency, and the design variable is the fiber orientation in the layers. The first-order shear deformation theory and the nine-node isoparametric finite element model are used for the finite element solution of the laminates. The modified feasible direction (MFD) method is used for the optimization routine. For this purpose, a program based on FORTRAN is used. Finally, the numerical analysis is carried out to investigate the effects of geometrical parameters and

boundary conditions on the optimal designs, and the results are compared.

2 Basic equations

Figure 1 shows a spherical shell of length a , width b , thickness h , and mean radius R . An orthogonal curvilinear coordinate system (x_1 , x_2 , and x_3) is considered to represent the geometry and deformation of the spherical shell when x_1 and x_2 axes are located in the midplane of the shell.

Considering the first-order shear deformation theory, the displacement fields are expressed as follows [9]:

$$\begin{aligned} u(x_1, x_2, x_3, t) &= u_0(x_1, x_2, t) + x_3 \psi_1(x_1, x_2, t) \\ v(x_1, x_2, x_3, t) &= v_0(x_1, x_2, t) + x_3 \psi_2(x_1, x_2, t) \\ w(x_1, x_2, x_3, t) &= w_0(x_1, x_2, t) \end{aligned} \quad (1)$$

where u_0 , v_0 , and w_0 are the midplane displacements and ψ_1 , ψ_2 are the rotations of the normal to midplane about the x_2 and x_1 axes, respectively.

The strain-displacement relations can be written as follows [9]:

$$\begin{Bmatrix} \varepsilon_1 \\ \varepsilon_2 \\ \gamma_{12} \end{Bmatrix} = \begin{Bmatrix} \frac{\partial u_0}{\partial x_1} + \frac{w_0}{R} \\ \frac{\partial v_0}{\partial x_2} + \frac{w_0}{R} \\ \frac{\partial u_0}{\partial x_2} + \frac{\partial v_0}{\partial x_1} \end{Bmatrix} + x_3 \begin{Bmatrix} \frac{\partial \psi_1}{\partial x_1} \\ \frac{\partial \psi_2}{\partial x_2} \\ \frac{\partial \psi_1}{\partial x_2} + \frac{\partial \psi_2}{\partial x_1} \end{Bmatrix}, \quad \begin{Bmatrix} \gamma_{23} \\ \gamma_{13} \end{Bmatrix} = \begin{Bmatrix} \frac{\partial w_0}{\partial x_2} - \frac{v_0}{R} + \psi_2 \\ \frac{\partial w_0}{\partial x_1} - \frac{u_0}{R} + \psi_1 \end{Bmatrix}, \quad (2)$$

The stress-strain relations for each layer of the laminated spherical shell can be written as:

$$\begin{Bmatrix} \sigma_1 \\ \sigma_2 \\ \tau_{12} \end{Bmatrix}_{(k)} = \begin{Bmatrix} \bar{Q}_{11} & \bar{Q}_{12} & \bar{Q}_{16} \\ \bar{Q}_{12} & \bar{Q}_{22} & \bar{Q}_{26} \\ \bar{Q}_{16} & \bar{Q}_{26} & \bar{Q}_{66} \end{Bmatrix}_{(k)} \begin{Bmatrix} \varepsilon_1 \\ \varepsilon_2 \\ \gamma_{12} \end{Bmatrix}_{(k)} \quad (3)$$

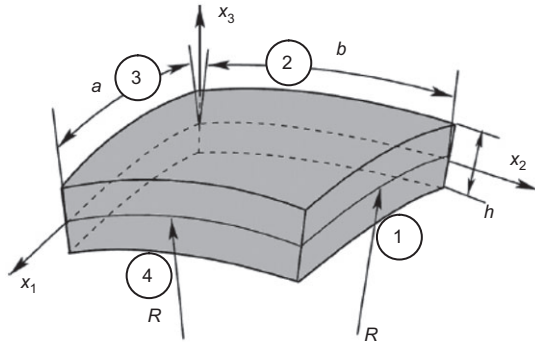


Figure 1 Geometry of a spherical shell [9].

$$\begin{Bmatrix} \tau_{23} \\ \tau_{13} \end{Bmatrix}_{(k)} = \begin{Bmatrix} \bar{Q}_{44} & \bar{Q}_{45} \\ \bar{Q}_{45} & \bar{Q}_{55} \end{Bmatrix}_{(k)} \begin{Bmatrix} \gamma_{23} \\ \gamma_{13} \end{Bmatrix}_{(k)} \quad (4)$$

where \bar{Q}_{ij} is the transformed reduced stiffness.

The stress resultants $\{N\}$, stress couples $\{M\}$, and transverse shear stress resultants $\{Q\}$ are:

$$\begin{Bmatrix} N_1 \\ N_2 \\ N_{12} \end{Bmatrix} = \int_{-h/2}^{h/2} \begin{Bmatrix} \sigma_1 \\ \sigma_2 \\ \tau_{12} \end{Bmatrix} dx_3, \quad \begin{Bmatrix} M_1 \\ M_2 \\ M_{12} \end{Bmatrix} = \int_{-h/2}^{h/2} \begin{Bmatrix} \sigma_1 \\ \sigma_2 \\ \tau_{12} \end{Bmatrix} x_3 dx_3, \quad \begin{Bmatrix} Q_1 \\ Q_2 \end{Bmatrix} = K \int_{-h/2}^{h/2} \begin{Bmatrix} \tau_{13} \\ \tau_{23} \end{Bmatrix} dx_3 \quad (5)$$

In Eq. (5), K is the shear correction factor. In this study, the shear correction factor is taken as $5/6$. The equations of motion in the absence of the applied load in terms of the stress resultants are given by Hamilton's principle as follows [9]:

$$\begin{aligned} N_{1,1} + N_{12,2} + \frac{Q_1}{R} &= I_{11} \ddot{u}_0 + I_{22} \ddot{\psi}_1 \\ N_{12,1} + N_{2,2} + \frac{Q_2}{R} &= I_{11} \ddot{v}_0 + I_{22} \ddot{\psi}_2 \\ M_{1,1} + M_{12,2} - Q_1 &= I_{22} \ddot{u}_0 + I_3 \ddot{\psi}_1 \\ M_{12,1} + M_{2,2} - Q_2 &= I_{22} \ddot{v}_0 + I_3 \ddot{\psi}_2 \\ Q_{1,1} + Q_{2,2} - \frac{N_1}{R} - \frac{N_2}{R} &= I_1 \ddot{w}_0 \end{aligned} \quad (6)$$

where the inertias I_i ($i=1, 2, 3, 11, 22$) are defined by:

$$\begin{aligned} (I_1, I_2, I_3) &= \int_{-h/2}^{h/2} \rho (1, x_3, x_3^2) dx_3 \\ I_{11} &= I_1 + \frac{2}{R} I_2, \quad I_{22} = I_2 + \frac{1}{R} I_3 \end{aligned} \quad (7)$$

3 Finite element formulation

In this study, a nine-noded Lagrangian rectangular shell element, which has five degrees of freedom (u , v , w , ψ_1 , ψ_2) is used for the finite element solution of the laminates. The interpolation of the displacement field is defined as:

$$\begin{Bmatrix} u \\ v \\ w \\ \psi_1 \\ \psi_2 \end{Bmatrix} = \sum_{i=1}^n N_i d_i \quad (8)$$

where d_i and N_i are the nodal variables and the interpolation function, respectively. The free vibration analysis

involves determination of natural frequencies from the condition:

$$([K]-\lambda[M])\{u\}=0 \tag{9}$$

where $[K]$, $[M]$, and $\lambda=\omega^2$ are the stiffness matrix, mass matrix, and eigenvalue, respectively. Eq. (9) is a set of homogeneous linear equations in the unknown displacements $\{u\}$. For nontrivial solution, the determinant is equal to zero, and the eigenvalues correspond to natural frequencies of the laminated plates. The subspace iteration method is used for the frequency analysis. The obtained smallest natural frequency (fundamental frequency) is used as an objective function and will be designed to maximize its value in the present optimization problem.

4 Modified feasible direction method

The MFD method is one of the most powerful methods for optimization problems. This method takes into account not only the gradients of objective function and constraints but also the search direction in the former iteration. In this study, there is no constraint.

Figure 2 shows the iterative process within each optimization process [11]. In Figure 2, X^q and X^{q+1} are the design variable vectors in two consecutive cycles of iteration. The procedure starts with an initial design vector, X^0 , i.e., $q=0$, $q=q+1$, and the objective function $F(X_i)$, is evaluated. $\nabla F(X_i)$, the gradients of objective function with respect to the design variable, is calculated using the finite difference method. A search direction S^q , is determined, and a one-dimensional search is made to find α . The above procedure is repeated with the new design vectors, until the

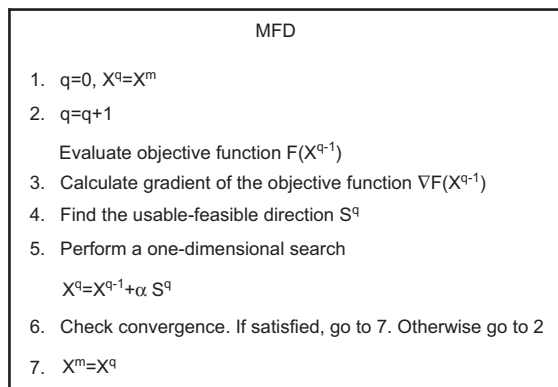


Figure 2 Flow chart of the MFD method.

design satisfies the optimality conditions or some other termination criterion.

The objective function $F(X_i)$ is accurately modeled as a quadratic polynomial approximation around the current iterate X_i as in Eq. (10):

$$F(X_i)=a_0 + \sum_{i=1}^{N_d} a_i X_i + \sum_{i=1}^{N_d} b_i X_i^2 \tag{10}$$

where N_d and X_i are the number of design variables and i th design variable, respectively. a_i and b_i are the coefficients of polynomial function determined by a least squares regression. After the objective function is approximated, their gradients with respect to the design variables are calculated by the finite difference method. The solving process is iterated until convergence is achieved.

Convergence or termination checks are performed at the end of each optimization loop. The optimization process continues until either convergence or termination occurs. The process may be terminated before convergence in two cases:

- The number of design sets so far exceeds the maximum number of optimization loops.
- If the initial design is infeasible and the allowed number of consecutive infeasible designs has been exceeded.

The optimization problem is terminated if all of the following conditions are satisfied:

- The current design is feasible,
- Changes in the objective function F :
 - a. The difference between the current value and the best design so far is less than the tolerance τ_F .

$$|F_{\text{current}} - F_{\text{best}}| \leq \tau_F$$

- b. The difference between the current value and the previous design is less than the tolerance,

$$|F_{\text{current}} - F_{\text{current-1}}| \leq \tau_F$$

- Changes in the design variables X^i :
 - a. The difference between the current value of each design variable and the best design so far is less than the respective tolerance τ^i .

$$|X_{\text{current}}^i - X_{\text{best}}^i| \leq \tau^i$$

- b. The difference between the current value of each design variable and the previous design is less than the respective tolerance,

$$|X_{\text{current}}^i - X_{\text{current-1}}^i| \leq \tau^i$$

The optimization process is resolved to obtain the global maximum from different initial points to check if other solutions are possible. The convergence tolerance ratio is considered 0.01 for the objective function.

5 Optimization problem

The objective of the design problem is to maximize the fundamental frequency of the laminated spherical shells. The fiber orientation is taken as a design variable. The optimization of the problem is formulated as:

Find: θ
 Maximize: $\omega_1 = \omega_1(\theta)$
 Subjected to: $0^\circ \leq \theta_k \leq 90^\circ, \Delta\theta = 1^\circ$ (11)

The fundamental frequency ω_1 for a given fiber orientation is determined from the finite element solution of the eigenvalue problems given by Eq. (9). The optimization procedure involves the stages of evaluating the fundamental frequency and improving the fiber orientation θ to maximize ω_1 . Thus, the computational solution consists of successive stages of analysis and optimization until a convergence is obtained, and the optimum fiber orientation θ_{opt} is determined within a specified accuracy.

6 Numerical results and discussion

6.1 Validation and convergence of the present study

In order to verify the efficiency of the present study, the results are compared with the literature results obtained for the laminated square spherical shell as shown in Tables 1 and 2. In the first example, free vibration of a simply supported cross ply (0°/90°) spherical shell is investigated (a=100 mm, b=100 mm, R=300 mm, h=1 mm). The following material properties are considered:

$E_1 = 25 \times 10^6$ Pa, $E_2 = 1 \times 10^6$ Pa, $G_{12} = G_{13} = 5 \times 10^5$ Pa, $G_{23} = 2 \times 10^6$ Pa, $\nu_{12} = 0.25$, $\rho = 1$ g/mm³

Fundamental frequency	[10]	Present study
ω (Hz)	0.73215	0.72589

Table 1 Convergence study of the present study for a simply supported cross ply (0°/90°) square spherical shell.

Nondimensional fundamental frequency	[6]	[12]	Present study
$\bar{\omega}$	47.332	47.109	46.974

Table 2 Comparison of the present study for a simply supported cross ply (0°/90°)₄ square spherical shell.

As can be seen from Table 1, the result obtained for free vibration in this present study is in very close agreement with the literature result.

In the second example, the free vibration of a simply supported cross ply (0°/90°)₄ spherical shell is investigated. The non-dimensional fundamental frequency is defined as:

$\bar{\omega} = \omega b^2 (\rho/E_2 h^2)^{1/2}$ (12)

Table 2 reveals that the result of the present study is close to the results in the literature.

6.2 Optimization problem

In this study, the optimization problem is solved for four-layered angle-ply symmetric (θ /- θ /- θ / θ) laminated spherical shells. Each of the lamina is assumed to be of the same thickness. The optimization results are given for T300/5208 graphite/epoxy material. The material properties are given as follows:

$E_1 = 181$ GPa, $E_2 = 10.3$ GPa, $G_{12} = G_{13} = 7.17$ GPa, $G_{23} = 2.39$ GPa, $\nu_{12} = 0.28$, $\rho = 1600$ kg/m³

In this study, the effect of the shell aspect ratio (a/b) on the optimum results is investigated for the simply supported angle-ply spherical shell (R/b=10, b/h=10). As seen in Figure 3, as shell aspect ratio increases, the maximum fundamental frequency diminishes because of the decrease in the shell stiffness.

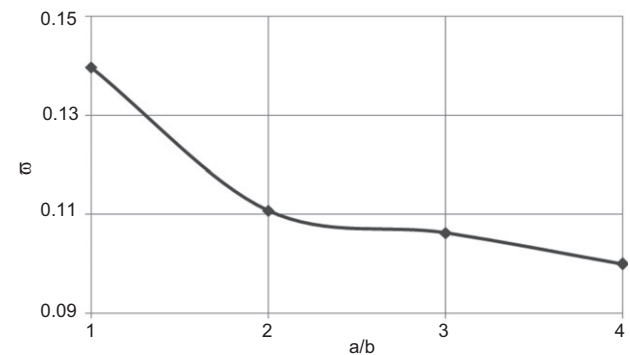


Figure 3 Effect of the shell aspect ratio on the fundamental frequency for simply supported square laminated spherical shells.

a/b	θ_{opt} (°)
1	45
2	0
3	9
4	16

Table 3 Effect of a/b ratio on the optimum fiber orientations for simply supported laminated spherical shells.

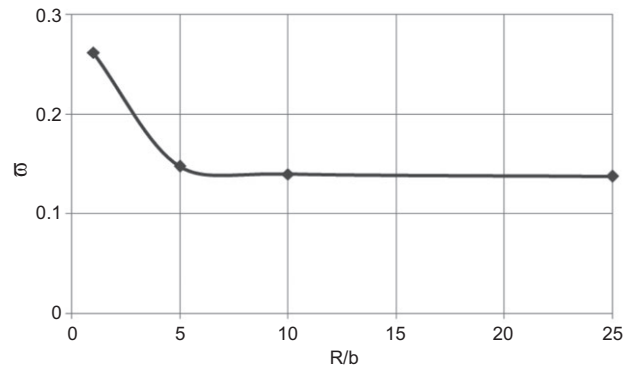


Figure 4 Effect of the curvature ratio on the fundamental for simply supported square laminated spherical shells.

In Table 3, the optimum fiber orientations are given for the shell aspect ratios for the simply supported square laminated spherical shells.

In this study, the effect of the curvature ratio (R/b) on the optimum results is investigated for the simply supported square angle-ply spherical shell ($b/h=10$). As seen in Figure 4, the maximum fundamental frequency decreases as curvature ratio increases. This is due to the fact that with the decrease of the curvature, the shell stiffness decreases. Also, the effect of the curvature ratio becomes more pronounced for $R/b < 10$. On the other hand, the optimum fiber orientations are obtained, $\theta_{opt} = 45^\circ$, for all curvature ratios.

In this study, different combinations of free (F), simply supported (S), and clamped (C) boundary conditions are implemented at the four edges of the plate. In particular, four different combinations are studied, namely, (SSSS), (CCCC), (CSCS), and (CFCF), where the first letter refers to the first plate edge, and the others follow in the anti-clockwise direction as shown in Figure 1. The effect of

Boundary conditions	ω	θ_{opt} (°)
(SSSS)	0.1396	45
(CCCC)	0.2046	0
(CSCS)	0.1976	0
(CFCF)	0.1922	0

Table 4 Effect of boundary conditions on the optimum results for laminated square spherical shells.

boundary conditions on the optimum results is investigated for a simply supported square angle-ply spherical shell ($R/b=10$, $b/h=10$). As seen in Table 4, the maximum and minimum fundamental frequencies occur for (CCCC) and (SSSS) boundary conditions, respectively. This is due to the fact that higher constraints at the edges increase the flexural rigidity of the spherical shell.

7 Conclusions

This paper deals with the frequency optimization of symmetrically laminated angle-ply spherical shells. The design objective is the maximization of the fundamental frequency, and the design variable is the fiber orientation in the layers. Initially, preliminary studies have been carried out by solving problems given in the literature for free vibration, and the results have been compared with the best known results available in the literature. Numerical results show that as the shell aspect ratio increases, the maximum fundamental frequency diminishes because of a decrease in the shell stiffness. The maximum fundamental frequency decreases as the curvature ratio increases. This is due to the fact that with the decrease in the curvature, the shell stiffness decreases. Also, the effect of the curvature ratio becomes more pronounced for $R/b < 10$. The curvature ratio has no effect on the optimum fiber orientations. The maximum and minimum fundamental frequencies occur for (CCCC) and (SSSS) boundary conditions, respectively. This is due to the fact that higher constraints at the edges increase the flexural rigidity of the spherical shell.

Received April 19, 2012; accepted May 29, 2012; previously published online July 13, 2012.

References

- [1] Narasimhan NC, Alwar RS. *J. Sound Vib.* 1992, 154, 515–529.
- [2] Xu CS, Chia CY. *Comp. Sci. Tech.* 1995, 54, 67–74.
- [3] Xu CS, Chia CY. *Acta Mech.* 1992, 94, 59–72.
- [4] Hashemi SH, Atashipour SR, Fadaee M, Girhammar UA. *Arch. Appl. Mech.*, 2012, In Press.
- [5] Lee SY, Chung DS. *Finite Elem. Des.* 2010, 46, 247–256.

- [6] Nanda N, Bandyopadhyay JN. *Aircraft Eng. Aero. Tech.* 2008, 80, 165–174.
- [7] Stavsky Y, Greenberg JB. *J. Acoust. Soc. Am.* 2003, 113, 847–851.
- [8] Panda SK, Singh BN. *Int. J. Mech. Mater. Des.* 2010, 6, 175–188.
- [9] Hashemi SH, Fadaee M. *J. Sound Vib.* 2011, 330, 4352–4367.
- [10] Topal U. *Int. Symp. on Advances in Earthquake and Struct. Eng.*, Süleyman Demirel University, 2007, Isparta-Antalya, Turkey.
- [11] Topal U, Uzman Ü. *Thin-Walled Struct.* 2008, 46, 667–675.
- [12] Chakravorty D, Sinha PK, Bandyopadhyay JN. *J. Eng. Mech.* 1998, 124, 1–8.